### Title
Nitrosyl-cobinamide (NO-Cbi), a new nitric oxide donor, improves wound healing through cGMP/cGMP-dependent protein kinase




### Journal
Cellular Signalling, 25(12)

### ISSN
0898-6568



### Authors
Spitler, Ryan
Schwappacher, Raphaela
Wu, Tao
et al.



### Publication Date
2013-12-01

### DOI
10.1016/j.cellsig.2013.07.029

Cellular Signalling 25 (2013) 2374–2382

Contents lists available at ScienceDirect

Cellular Signalling

journal homepage: www.elsevier.com/locate/cellsig

# Nitrosyl-cobinamide (NO-Cbi), a new nitric oxide donor, improves wound healing through cGMP/cGMP-dependent protein kinase

Ryan Spitler [a,*], Raphaela Schwappacher [b], Tao Wu [c], Xiangduo Kong [a], Kyoko Yokomori [a], Renate B. Pilz [b], Gerry R. Boss [b], Michael W. Berns [a,b]

[a] University of California Irvine, Irvine, CA, United States
[b] University of California San Diego, La Jolla, CA, United States
[c] Harvard Medical School, Massachusetts General Hospital, Boston, MA, United States

ARTICLE INFO

*Article history:*
Received 8 May 2013
Received in revised form 10 July 2013
Accepted 22 July 2013
Available online 3 August 2013

*Keywords:*
Nitric oxide
Wound healing
Cell migration
PKG
ERK
Src

ABSTRACT

Nitric oxide (NO) donors have been shown to improve wound healing, but the mechanism is not well defined. Here we show that the novel NO donor nitrosyl-cobinamide (NO-Cbi) improved *in vitro* wound healing in several cell types, including an established line of lung epithelial cells and primary human lung fibroblasts. On a molar basis, NO-Cbi was more effective than two other NO donors, with the effective NO-Cbi concentration ranging from 3 to 10 μM, depending on the cell type. Improved wound healing was secondary to increased cell migration and not cell proliferation. The wound healing effect of NO-Cbi was mediated by cGMP, mainly through cGMP-dependent protein kinase type I (PKGI), as determined using pharmacological inhibitors and activators, and siRNAs targeting PKG type I and II. Moreover, we found that Src and ERK were two downstream mediators of NO-Cbi's effect. We conclude that NO-Cbi is a potent inducer of cell migration and wound closure, acting *via* cGMP, PKG, Src, and extracellular signal regulated kinase (ERK).



## 1. Introduction

Nitric oxide (NO) and NO donors such as sydnonimines, diazeniumdiolates, S-nitrosothiols, and NO-containing nanoparticles have been shown to improve wound healing to varying degrees [1,2]. These agents have been studied *in vitro*, in airway and gastric epithelial wounds [3,4], and *in vivo*, in diabetic ulcers [5], and skin abscesses [6]. Yet, the molecular basis for the effect of NO donors in wound healing is poorly defined, and a better understanding of how NO functions to improve wound healing is needed.

NO is a gaseous signaling molecule that can have multiple molecular/biochemical effects including reaction with metalloenzymes [7], generation of reactive nitrogen species [8], formation of nitrosothiol groups [9], and nitration of protein tyrosine residues [10]. All of these reactions can have further secondary effects on a variety of signaling pathways that can translate to multiple and sometimes divergent physiologic effects. Thus, NO can be pro-proliferative/anti-apoptotic or anti-proliferative/pro-apoptotic depending on the cell type [11–13]. A key signaling pathway activated by NO, and where NO was first discovered to have a physiologic effect, is the guanylate cyclase/cGMP/cGMP-dependent protein kinase (PKG) pathway [14]. NO activates soluble guanylate cyclase, which increases the intracellular cGMP concentration; cGMP has several target proteins including PKG, phosphodiesterases (PDEs), and membrane ion channels [14]. PKG can phosphorylate enzymes, structural proteins, and transcription factors, and, thus, can initiate diverse metabolic and structural changes, and alterations in gene expression [14,15]. We and others have reported that PKG can activate the extracellular signal regulated kinase (MEK/ERK) signaling pathway [16,17], and we have shown recently that PKG can activate Src upstream of MEK/Erk [18]. The two isoforms of PKG, type I and type II, are transcribed from two separate genes and have different cellular locations and target proteins [19].

In the work reported here, we study *in vitro* wound healing in several different cell types. The new direct NO-releasing compound nitrosyl-cobinamide (NO-Cbi) is compared to two established direct NO donors. The parent compound of NO-Cbi is cobinamide, a structural analog of cobalamin (vitamin $B_{12}$) lacking its dimethylbenzimidazole group. This imparts several chemical differences between cobinamide and cobalamin, most notably that cobinamide has higher affinity for ligands, including NO. Thus, cobinamide can be used as an NO scavenger, while NO-Cbi can be used as an NO donor [20–23]. In this paper we report results of NO-Cbi in a cellular based wound-healing model using a robotic system for generating uniform scratch wounds and a software developed specifically for assessing the results. We found that NO-Cbi significantly enhanced wound healing *via* increased cell

*Abbreviations:* NO, Nitric oxide; NO-Cbi, nitrosyl-cobinamide; PKG, cGMP-dependent protein kinase; ERK, extracellular signal regulated kinase; PDE, phosphodiesterase; SNP, sodium nitroprusside.

* Corresponding author at: Department of Developmental & Cell Biology, University of California Irvine, Beckman Laser Institute, 1002 Health Sciences Rd, Irvine, CA 92612, United States. Tel.: +1 949 824 7859; fax: +1 949 824 8413.
*E-mail address:* rspitler@uci.edu (R. Spitler).

0898-6568/$ – see front matter © 2013 Elsevier Inc. All rights reserved.
http://dx.doi.org/10.1016/j.cellsig.2013.07.029

migration as opposed to cell proliferation, and that its effects were mediated *via* cGMP/PKG, and Src and ERK.

## 2. Material and methods

### 2.1. Cell culture

The following three cell lines were obtained from the American Type Tissue Culture Collection (ATCC, Rockville, MD): A549 adenocarcinoma human alveolar epithelial cells, U2OS human osteosarcoma cells, and PtK2 rat kangaroo renal epithelial cells. In addition to these established cell lines, normal human lung fibroblasts (NHLF, used between passages 3–7), were obtained from Lonza (Basel, Switzerland). Cells were grown in T-75 flasks (Corning, Fisher, Pittsburgh, PA) in a 37 °C, 5% $CO_2$/95% air incubator in the following media: A549 and U2OS cells in Dulbecco's Modified Eagle's Medium (DMEM), NHLF cells in F12-K medium, and PtK2 cells in Modified Eagle's Medium (MEM); all three media were supplemented with 10% fetal bovine serum (Mediatech, Manassas, VA). For wound healing experiments, cells were trypsinized with TrypLE (Invitrogen Life Technologies, Carlsbad, CA), seeded into 6-well plates (Corning, Fisher, Pittsburgh, PA) or 35 mm fluorodish culture dishes (World Precision Instruments, Sarasota, Fl), and grown to confluency.

#### 2.1.1. Preparation of NO-Cbi

Cobinamide was produced by base hydrolysis of hydroxocobalamin (Sigma-Aldrich, St. Louis, MO) as described previously [24]. A cobinamide solution was thoroughly deoxygenated using argon, the cobalt was reduced from +3 to +2 valence state using a two-molar excess of ascorbic acid, and NO gas (99.99% pure, Matheson Gas Co.) was bubbled through the reduced cobinamide solution [25]. Concentrated stock solutions of NO-Cbi were diluted in deoxygenated sterile water, and the diluted NO-Cbi was added to cells using a Hamilton syringe (Hamilton, Reno, NV).

#### 2.1.2. Scratch wound closure assay

Scratch wounds in a cell monolayer were created robotically using a 200 μl pipette tip held in place with a mechanical arm. A computer-controlled automated stage moved the cells creating a uniform 20 mm long by 600–700 μm wide wound in the monolayer. The cells were then washed once with Hank's buffered saline solution (HBSS) to remove detached cells, and placed back in their standard culture medium. The open wound area was recorded for up to 72 h by one of the following two methods. Method (A): Images were imported into ImageJ (Wayne Rasband, NIH) where a region of interest was traced using the computer mouse. The wound margin and the wound area (in pixels) within the region of interest were digitally computed. Method (B): A MatLab program was written that automatically detected the wound margin and accurately mapped the change in wound area. The wound area was mapped using a script, which blurred the image and subtracted the blurred image from the original image. Smooth regions (such as the wound) have less difference between the blurred and original image, allowing generation of a clear wound boundary. When analyzing images of varying intensities, the program can be finely tuned by adjusting the threshold and blur-block parameters, which allows for an accurate measurement. The wound closure rate was determined by plotting changes in wound area as a function of time.

#### 2.1.3. Nitric oxide donor treatments

Three different direct NO donors were used: NO-Cbi, Deta-NONOate (Cayman Chemical, Ann Arbor, MI), and sodium nitroprusside (SNP, Sigma-Aldrich). Based upon preliminary experiments, for optimal wound closure, cells were treated as follows at the noted times post wounding: A549 cells—5 μM of each NO donor at 0, 4, 9, and 24 h; PtK2 cells—10 μM NO-Cbi at zero time; NHLF cells—3 μM NO-Cbi at 0, 6, 30 and 54 h; and U2OS cells—5 μM NO-Cbi at 0, 2, and 5 h. The migration response of each cell type was measured between 24–78 h, depending on the cell type.

#### 2.1.4. Microscopy

Fluorescent and phase contrast images were captured through a 10–32x magnification Ph1 objective on an inverted microscope (Axiovert 135, Zeiss, Jena, Germany) with a ORCA-$R^2$ charge-coupled device (CCD) camera (Hamamatsu, Bridgewater, NJ). Images were acquired using Robolase II software, an integral element of the automated Robolase system we developed previously [26]. The microscope stage was modified to accommodate a multi-well format for high-throughput analyses.

#### 2.1.5. Transwell migration assay

A549 cells were serum-starved for 4 h prior to seeding $10^4$ cells in 100 μl of DMEM/0.1% FBS in the top chamber of a 24-well transwell plate with an 8.0 μm pore polycarbonate membrane (Corning, Fisher); DMEM/10% FBS was placed in the bottom chamber. Cells received 5 μM NO-Cbi for 1 h immediately after initiating serum starvation, and again when they were seeded in the top chamber. After 24 h, the cells were fixed in 70% cold ethanol and a cotton swab was used to remove cells remaining on top of the membrane. Cells were stained using bisbenzimide H 33342 trihydrochloride (Hoechst, Invitrogen Life Technologies), and visualized as described above. Images were imported into ImageJ, and a cell counter plug-in was used to count cells. Six random images were taken for each replicate to determine representative cell counts. The coordinates of each image were noted to ensure that different regions within the same membrane were sampled.

#### 2.1.6. Mitotic index

The mitotic index was determined in two different cell types by two different methods. A549 cells were fixed in cold 70% ethanol and permeabilized using PBS/0.2% Triton X-100. Mitotic cells were identified using phospho-histone H3 (Ser10) rabbit primary antibody (H3S10, Cell Signaling Technology, Danvers, MA) incubated at 1:1000 dilution in PBS/5% BSA; total cells numbers were determined using Hoechst 33342 added at 1:3000 dilution in PBS to mark nuclei. Images were analyzed using ImageJ.

PtK2 cells were transfected with a nuclear-targeted green fluorescent protein fusion construct (NBS1-GFP), to detect GFP-positive, dividing cells; the cells were observed for 15 h using time-lapse microscopy at 37 °C to record mitotic events. The mitotic index was calculated from 100 to 150 cells per field [27].

#### 2.1.7. MTS cell proliferation assay

A549 cells were seeded at $5 \times 10^3$ cells per well in a 96-well plate and were incubated overnight to allow cell attachment. The cells were then treated with either PBS or 5 μM NO-Cbi at 0, 4 and 9 h. At 24 h the level of cell proliferation was determined using a MTS (3-(4,5-dimethylthiazol-2-yl)-5(3-carboxymethoxyphenyl)-2-(4-sulfophenyl)-2H-tetrazolium) cell proliferation assay (CellTiter 96® $AQ_{ueous}$ Non-Radioactive Cell Proliferation Assay; Promega, Madison, WI) according to the manufacturer's instructions. The absorbance was measured at a wavelength of 490 nm and plotted for both untreated and treated cells.

#### 2.1.8. Cell velocity determination

A549 cells were seeded at $4.5 \times 10^6$ per 35 mm fluorodish 24 h prior to the experiment. Cells were then treated with either PBS or 5 μM NO-Cbi at 0 and 4 h. Cell migration was monitored for 16 h after automated scratching (as described above) using time-lapse microscopy [IX8I, Olympus; equipped within an incubation chamber (37 °C and 5% $CO_2$)] and an interval of 1 h. The centroid of individual cells

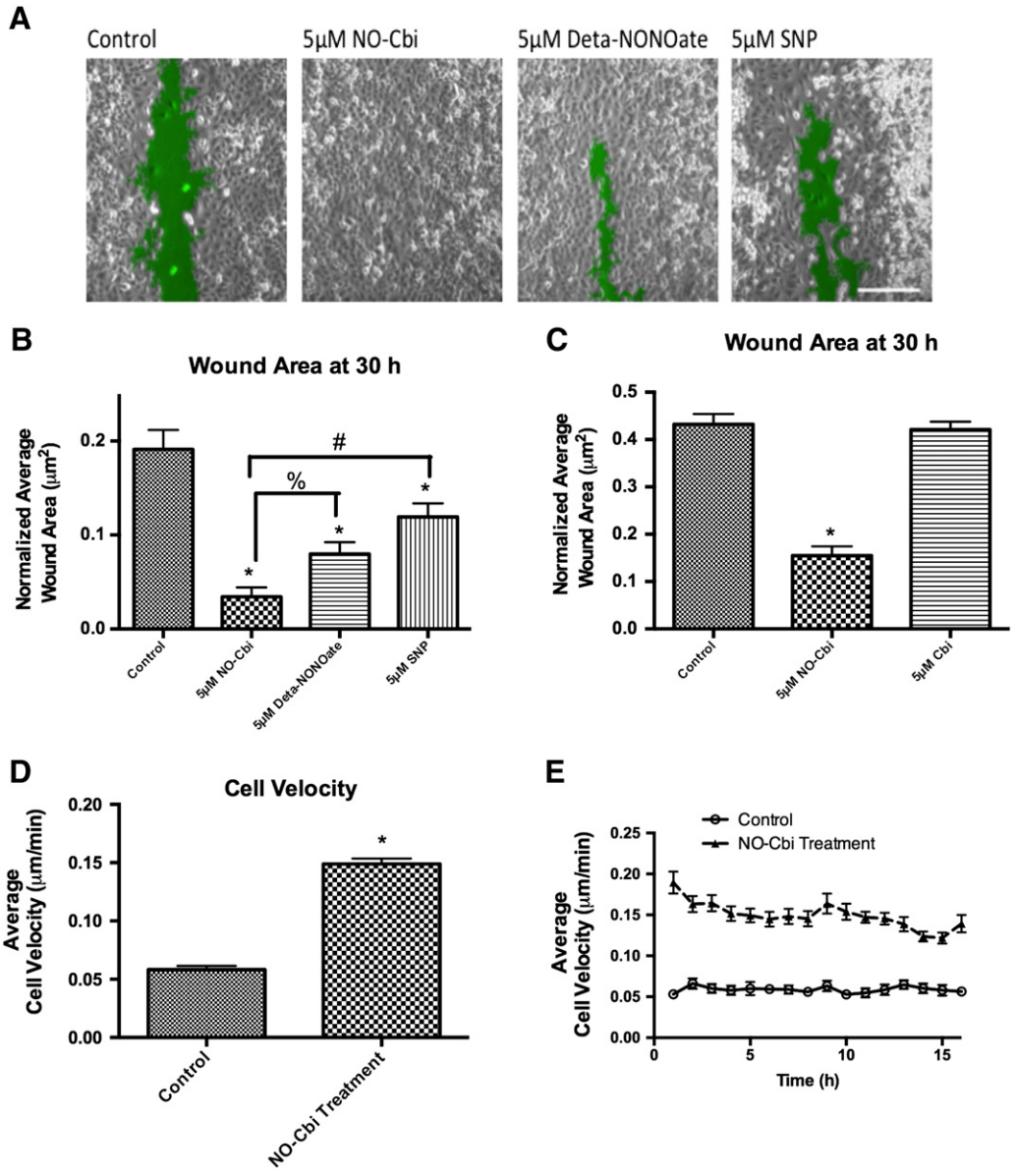


**Fig. 1.** NO-Cbi increases wound healing in A549 cells. (A and B) Mechanical scratch wounds were generated in a monolayer of A549 cells, and 30 h later, the area of the wound was evaluated by a computer-based system as described in Material and methods. At 0, 4, 9, and 24 h post-wounding, cells received fresh medium with 5 μM of NO-Cbi, Deta-NONOate, sodium nitroprusside (SNP), or fresh medium alone. The normalized average wound area was determined by dividing the final wound area by the initial wound area and averaging replicates. The green area marks the wound. Bar, 100 μm. (C) Cells were treated as in Panel B with 5 μM NO-Cbi or 5 μM cobinamide (Cbi), the parent molecule of NO-Cbi. (D) Cells were treated with 5 μM NO-Cbi at 0 and 4 h and tracked for a period of 16 h post-wounding. Individual cell tracks were recorded and used to calculate the average velocity of the cells at the wound margin. The total average velocity was then plotted for NO-Cbi treated cells compared to control cells. (E) The average velocity was also calculated for each hour from the data obtained in panel D, the treatment compared to control average velocities at each timepoint were found to be statically significant $p < 0.0001$. Data represent the mean ± SEM of at least 3 separate experiments with $n = 12$ (A, B and C); $n = 68$ for control and $n = 97$ for NO-Cbi treated cells (D and E); $^{*}p < 0.001$ compared to control, $^{\#}p < 0.01$ and $^{\%}p < 0.05$ for the indicated comparison.

was tracked in acquired images using Fiji software (open source image processing package based on ImageJ) and a manual cell tracking plug-in. The instantaneous velocity (μm/min) was calculated between each point of centroid movement as the distance divided by time. The summations of instantaneous velocities were averaged to determine an overall mean velocity for each track. The summation of all respective tracks was averaged giving the total average velocity for each experimental condition.

### 2.1.9. Measurement of cGMP

A cyclic GMP EIA kit (Cayman Chemical Company, Arbor, MI) was used to measure the cGMP concentration in cell lysates. Cells were serum-starved for 3 h in DMEM/0.1% FBS before being treated with the indicated agents, and processed according to the manufacturer's protocol.

### 2.2. Pharmacological treatments

Cells were treated with the following drugs: 10 μM 1H-[1,2,4]oxadiazolo[4,3-a]quinoxalin-1-one (ODQ, an inhibitor of soluble guanylate cyclase; Cayman Chemical) or 50 μM 1-methyl-3-isobutylxanthine (IBMX, a non-specific phosphodiesterase inhibitor; Cayman Chemical) for 1 h; 1 μM vardenafil (a phosphodiesterase V inhibitor; Toronto Research Chemicals, Toronto, Canada), 1 μM Rp-8-pCPT-cGMPS (a PKG inhibitor; BioLog, Farmingdale, NY), 25 μM 8-pCPT-cGMPS (a membrane-permeable form of cGMP that

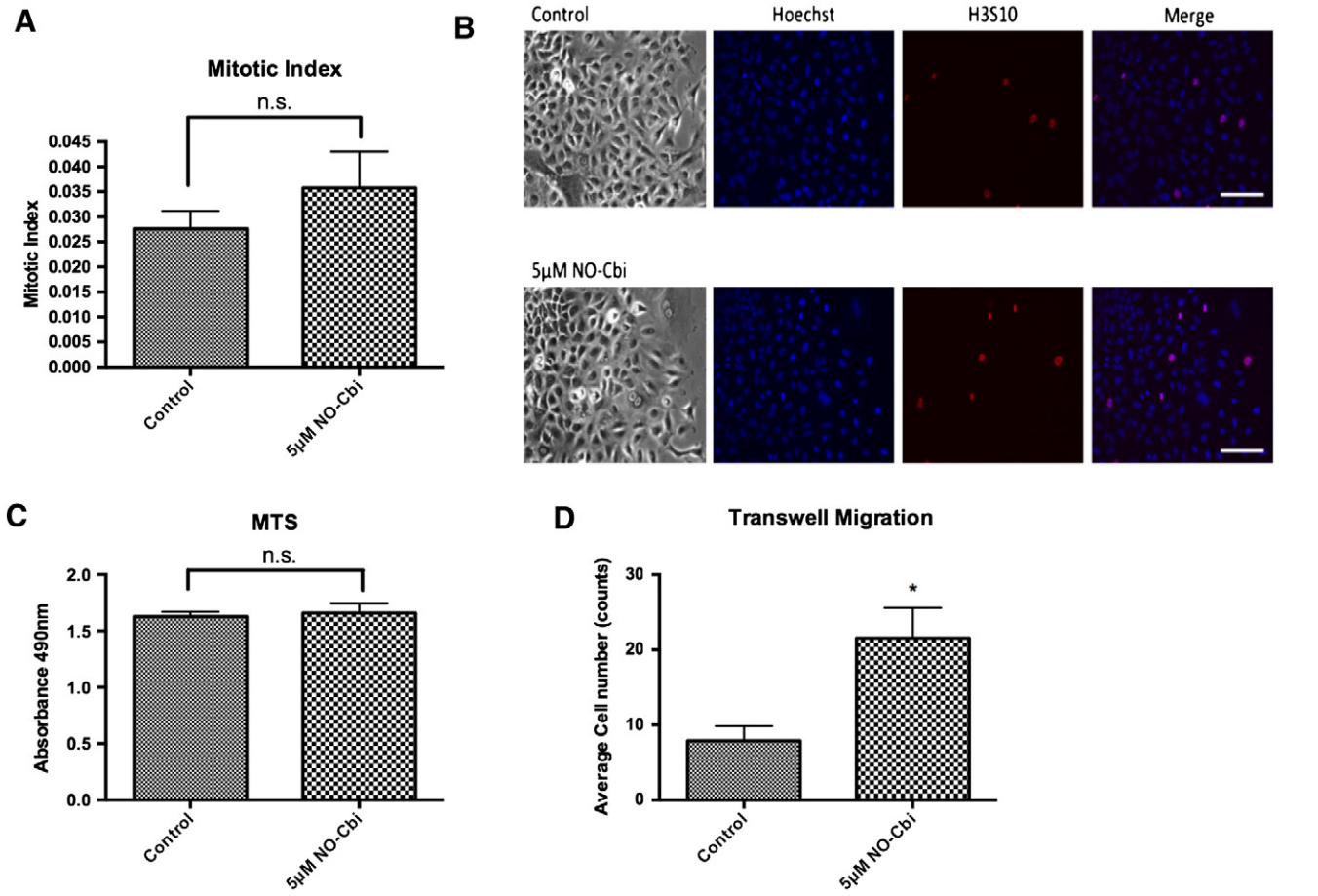


**Fig. 2.** NO-Cbi increases cell migration but not proliferation. (A and B) Cells were stained with antibody specific for histone H3 phosphorylated on Ser10 (H3S10) to identify mitotic cells (red); nuclei were counterstained with Hoechst 33342 (blue). Photographs in B were analyzed using the cell counter ImageJ plugin to calculate a mitotic index. Bar, 100 μm. (C) A549 cells were treated with 5 μM NO-Cbi at 0, 4 and 9 h, and cell proliferation was measured at 24 h as described in Material and methods. (D) A549 cells were pre-treated with 5 μM NO-Cbi, seeded onto a polycarbonate membrane, and treated again with 5 μM NO-Cbi. Transwell migration was quantified after 24 h as described in Material and methods. Data represent the mean ± SEM of at least 3 separate experiments with n = 3 fields of view (A) and n = 8 (C) in each experiment; $^{*}p < 0.001$ compared to control, n.s. (not significant).

activates PKG; BioLog), or 5 μM 8-CPT-cAMP (an activator of both cAMP-dependent protein kinase (PKA) and PKG, and of EPAC; BioLog) added at 0, 4, 9 and 24 h; or 10 μM PP2 or PP3 (a Src-specific inhibitor and its non-functional analog, respectively; Cayman Chemical) or 5 μM U1026 (a MEK-specific inhibitor, Promega; Madison, WI) for 30 h.

*2.2.1. siRNA-mediated PKGI and PKGII knockdown*

A549 cells were transfected with 100 pmol of siRNA oligoribonucleotides per 6-well dish using Lipofectamine 2000 (Invitrogen Life Technologies) according to the manufacturer's protocol. PKGI and PKGII expression was specifically reduced using predesigned oligoribonucleotides (SI02758630 for human PKGI and SI102224103 for human PKGII; Qiagen, Valencia, CA); a siRNA targeting GFP was used as a control.

*2.2.2. RT-qPCR*

RNA was isolated from A549 cells using the RNeasy kit (Qiagen), and cDNA was reverse-transcribed using the RT$^2$ First strand kit (Qiagen). qPCR was performed using a RT$^2$ SYBR green qPCR master mix (Qiagen) and gene specific primers for human PKGI (forward 5′-TGGACACAAGACAGCAGGAG-3′ and reverse 5′-TCCCTGAGAATGGTCC AGAG-3′), human PKGII (forward 5′-ACAAACCCCCTGAATTTTCC-3′ and reverse 5′-TGGTTTCCTGGTTCTCCTTG-3′), and human GAPDH (forward 5′-AACGGATTTGGTCGTATTGGG-3′ and reverse 5′-TGGAAGATGGTGAT GGGATTTC-3′).

*2.2.3. Western blots*

Cells were lysed and harvested in Laemmli buffer heated to 100 °C (BioRad, Hercules, CA). Lysates were sonicated and resolved on a SDS–PAGE gel, and proteins were transferred onto a nitrocellulose membrane (LI-COR Biosciences, Lincoln, NE). The membranes were blocked for 1 h with TBS/5% BSA, and incubated overnight with antibodies specific for phospho-VASP(Ser239) at 1:1000, phospho-Src(Tyr416) at 1:500, or phospho-ERK1/2(Thr202/Tyr204) at 1:10,000 in TBS/5% BSA (all antibodies from Cell Signaling Technology), or PKGI or PKGII antibodies (Abgent, San Diego, CA) at 1:500 in TBS/5% dry milk. Membranes were then incubated with an anti-rabbit-HRP antibody at 1:2000 for 1 h and developed using a luminol-based chemiluminescent substrate.

*2.2.4. Statistical analysis*

Data are presented as mean ± standard error of the mean (SEM). Student's t-tests were used for experiments that contained only two conditions, and a one-way analysis of variance (ANOVA) followed by Bonferroni's post-test was used for experiments containing three or more conditions. A p value $<0.05$ was considered to be statistically significant.

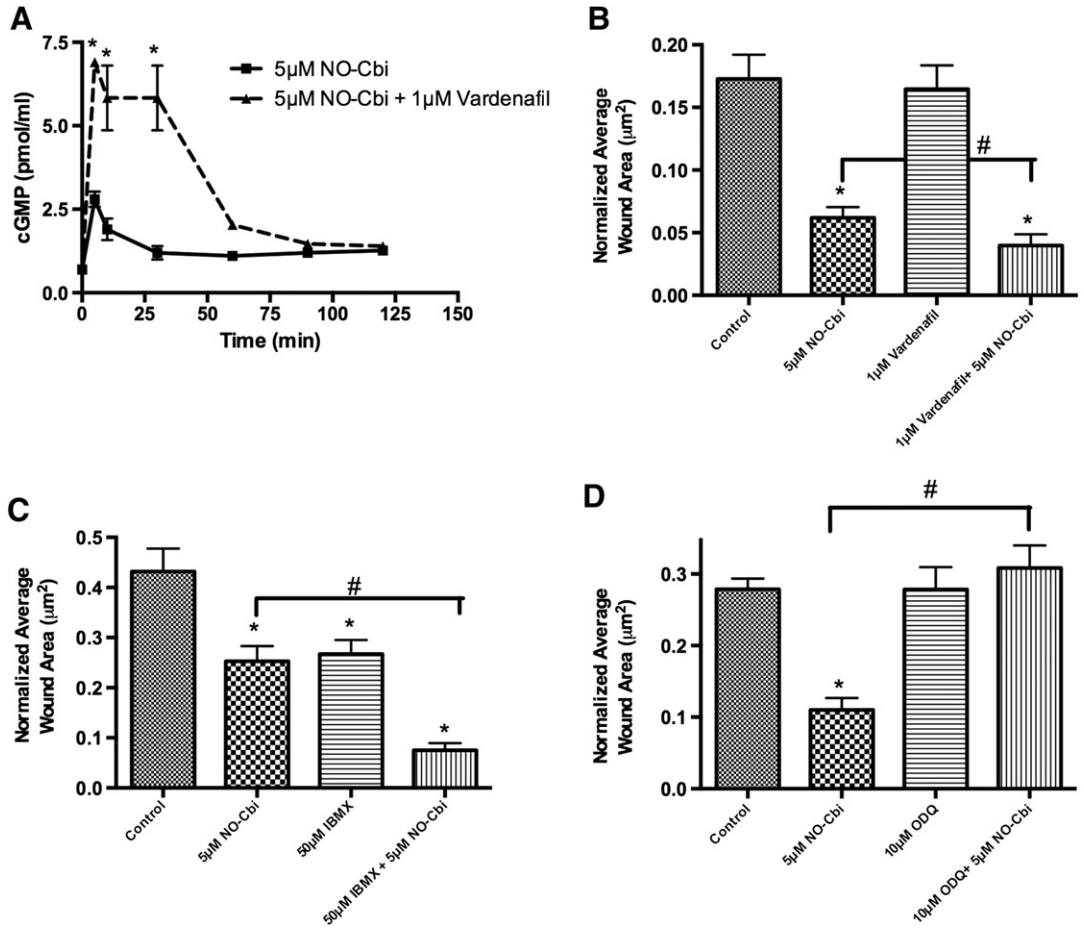


**Fig. 3.** NO-Cbi enhances wound healing through a cGMP-dependent mechanism. (A) Measurement of intracellular cGMP concentration in A549 cells after treatment with 5 μM NO-Cbi, in the presence (triangles, broken line) or absence (squares, solid line) of the PDE V inhibitor vardenafil (1 μM). (B) A549 cells were treated repeatedly with 5 μM NO-Cbi, and wound healing was measured after 30 h as described in Fig. 1A, but some cells received 1 μM vardenafil as indicated. (C) Cells were treated as in panel B, but the broad PDE inhibitor IBMX (50 μM) was added instead of vardenafil. (D) Cells were treated with NO-Cbi as in panel B, but some cells received the guanylate cyclase inhibitor ODQ (10 μM). Data represent the mean ± SEM of at least 3 separate experiments with n = 3 (A; $^{*}p < 0.001$ for NO-Cbi + vardenafil compared to NO-Cbi alone) and with n = 12 (B–D; $^{*}p < 0.001$ compared to control and $^{\#}p < 0.05$ for the indicated comparison).

## 3. Results

### 3.1. NO-Cbi enhances wound closure

NO-Cbi significantly enhanced wound closure in four different cell types. In A549, NHLF, and U2OS cells, 3–5 μM NO-Cbi added at 0, 4, 9, and 24 h post wounding provided maximal enhancement of wound closure (Figs. 1A, B and S1B, C). In PtK2 cells, a single application of 10 μM NO-Cbi significantly improved wound closure (Fig. S1A). NO-Cbi was compared to two other direct NO donors, DetaNONOate and sodium nitroprusside [3,28]. It performed better than either drug used at the same concentration and added at the same time (Fig. 1A, B). The parent compound cobinamide had no effect on wound closure (Fig. 1C). In addition, cell velocity of control and NO-Cbi-treated A549 cells was measured. NO-Cbi increased the average velocity of individual cells at the wound margin by almost three-fold (Fig. 1D, E and Videos S1 and S2), and induced the cells to move mostly as a sheet.

### 3.2. NO-Cbi effect on wound healing is mediated via cell migration rather than proliferation

We found that NO-Cbi did not significantly increase the mitotic index in either A549 or PtK2 cells (Figs. 2A, B and S2), and did not affect A549 proliferation (Fig. 2C). This, plus results on individual cell velocity described in the previous section, indicated that NO-Cbi stimulates cell migration, rather than cell multiplication, leading to enhanced wound closure. To confirm the effect of NO-Cbi on cell motility, we also performed transwell migration assays. NO-Cbi significantly increased migration of A549 cells through the membrane compared to control cells (Fig. 2D). Collectively, these results suggest that NO-Cbi improved wound healing primarily through inducing an increase in cell migration, with little effect on cell proliferation.

### 3.3. NO-Cbi positively affects wound closure through a cGMP-dependent mechanism

NO stimulates cGMP production by activating soluble guanylate cyclases [29]. Therefore, we exposed A549 cells to NO-Cbi for different times; additionally some cells were treated with the PDE V inhibitor vardenafil. The intracellular cGMP concentration increased about three-fold after treating the cells with 5 μM NO-Cbi for 5 min, and returned to near-basal concentrations after ~30 min (Fig. 3A). Combining NO-Cbi with vardenafil increased the cGMP concentration about two-fold compared to NO-Cbi alone; in addition, the cGMP concentration remained elevated longer, returning to the basal concentration at >80 min (Fig. 3A). Adding either vardenafil or IBMX, a broad-spectrum phosphodiesterase inhibitor, to NO-Cbi markedly enhanced wound healing (Fig. 3B, C); vardenafil alone had no effect, while IBMX alone significantly improved wound healing (Fig. 3B, C).

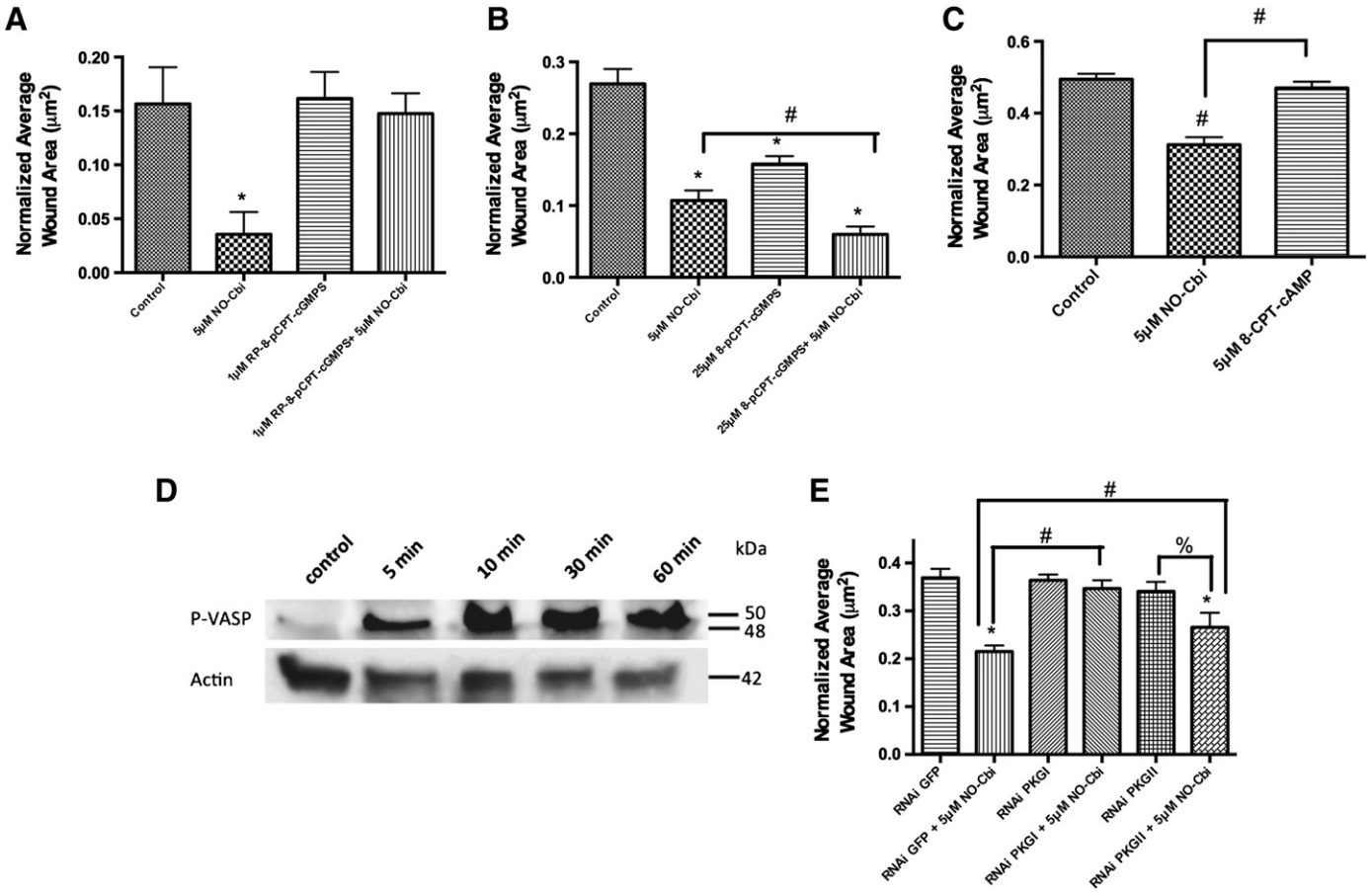


**Fig. 4.** PKG is necessary for NO-Cbi to enhance wound healing. (A and B) A549 cells were treated repeatedly with 5 μM NO-Cbi, and wound healing was measured after 30 h as described in Fig. 1A, but some cells received at the same times 1 μM RP-8-pCPT-cGMPS (A) or 25 μM of 8-pCPT-cGMP (B), as indicated. (C) A549 cells were treated repeatedly with 5 μM NO-Cbi or 8-CPT-cAMP. (D) A549 cells were treated with a single dose of NO-Cbi (5 μM) for the indicated time and cell lysates were analyzed by Western blotting with an antibody specific for VASP phosphorylated on Ser259, a preferred PKG phosphorylation site. Actin served as a loading control. (E) A549 cells were transfected with siRNAs targeting GFP (control), PKGI, or PKGII (specific mRNA knockdown and protein levels after siRNA treatment are shown in Supplemental Fig. S3). Data represent the mean ± SEM of at least 3 separate experiments with n = 12 (A and B; $^{*}p < 0.001$ compared to control, $^{\#}p < 0.05$ compared to NO-Cbi), n = 12 (C $^{\#}p < 0.001$ compared to control and indicated comparison) and n = 12 (E; $^{*}p < 0.001$ compared to GFP control, $^{\#}p < 0.001$ and $^{\%}p < 0.001$ for the indicated comparisons).

To determine whether the effects of NO-Cbi were mediated through cGMP, A549 cells were simultaneously treated with NO-Cbi and the guanylate cyclase inhibitor ODQ. By itself, ODQ had no effect on wound closure, but it inhibited NO-Cbi's enhancement of wound closure (Fig. 3D). Together, these data indicate that the positive effect of NO-Cbi on wound healing was through a cGMP-dependent mechanism.

### 3.4. PKG mediates enhanced wound healing induced by NO-Cbi

To determine if NO-Cbi was acting *via* PKG in enhancing wound healing, A549 cells were treated with the PKG-specific inhibitor RP-8-pCPT-cGMP. RP-8-pCPT-cGMPS treatment alone had no effect, but it completely prevented NO-Cbi's enhancement of wound healing (Fig. 4A). Inversely, the PKG-specific activator 8-pCPT-cGMP significantly improved wound healing in A549 cells, and augmented NO-Cbi-induced wound healing (Fig. 4B). These data provide evidence that NO-Cbi's effect on wound healing was mediated *via* PKG. We found no effect of 8-CPT-cAMP, an EPAC and cAMP-dependent protein kinase (PKA) and PKG activator, when used under the same conditions as NO-Cbi (Fig. 4C).

Consistent with NO-Cbi operating through a cGMP/PKG-dependent mechanism, NO-Cbi increased phosphorylation of vasodilator-stimulated phosphoprotein (VASP) at Ser239, a preferential phosphorylation site for PKG [30], in A549 cells (Fig. 4D). Peak phosphorylation began at 10 min and remained elevated for up to 60 min.

To determine which PKG isoform was mediating the effect of NO-Cbi, A549 cells were treated with siRNAs targeting PKGI or PKGII. PKGI knockdown completely inhibited NO-Cbi's acceleration of wound healing, while treatment with PKGII siRNA only partially blocked the effect of NO-Cbi (Fig. 4E). PKG siRNA transfection in unstimulated cells did not significantly affect wound healing. The knockdown efficiencies of PKGI and II siRNAs were ~60% and ~80%, respectively (Fig. S3). These findings demonstrate that the positive effect of NO-Cbi depends on PKG, most notably on PKGI.

### 3.5. NO-Cbi effect on wound healing proceeds through Src and ERK

Because Src and ERK are known to be involved in cell migration [31], and we previously demonstrated that Src and ERK are activated downstream of PKG [32], we assessed if they were involved in NO-Cbi enhancement of wound healing. Time-course experiments in A549 cells revealed that phosphorylation of Src and ERK markedly increased after 5 min of NO-Cbi stimulation, indicating activation of both pathways (Fig. 5A, B). The Src inhibitor PP2 and the MEK/ERK inhibitor U0126 completely prevented NO-Cbi-induced enhancement of wound healing in A549 cells (Fig. 5C, D). Neither agent alone had an effect on wound healing in the absence of NO-Cbi. In addition, PP3, a non-active PP2 analog, did not inhibit the effect of NO-Cbi on wound healing

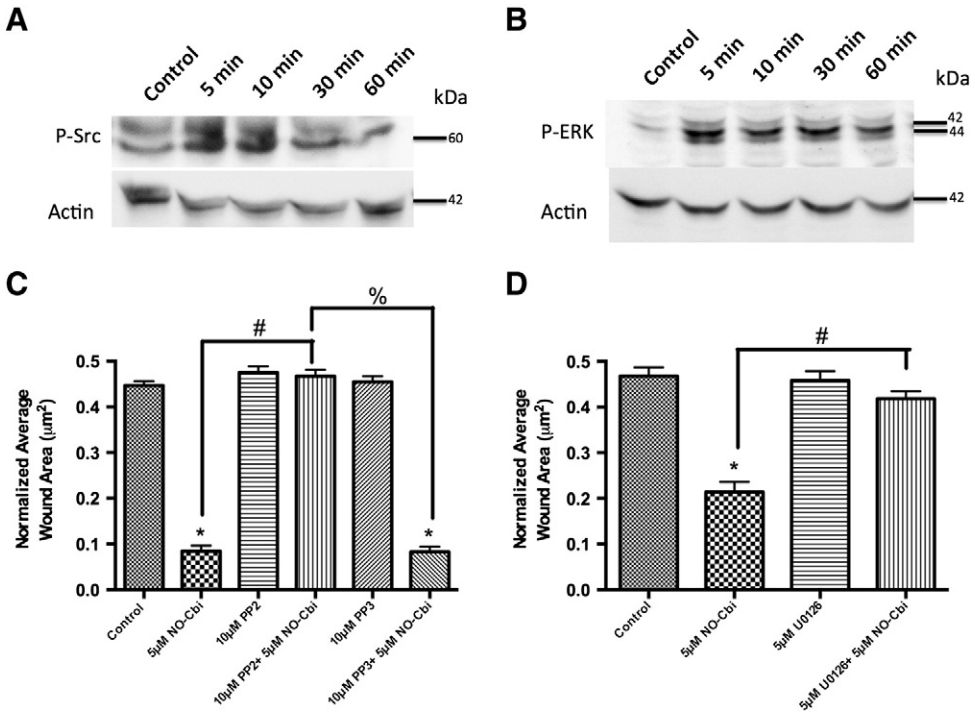


**Fig. 5.** Src and MEK/ERK are required for NO-mediated wound healing. (A and B) A549 cells were treated with a single dose of NO-Cbi (5 μM) for the indicated times and cell lysates were analyzed by Western blotting with an antibody specific for Src phosphorylated on Tyr416 (A) or ERK phosphorylated on Thr202/Tyr204 (B). Actin served as a loading control. (C) A549 cells were repeatedly exposed to 5 μM NO-Cbi, and wound healing was measured after 30 h as described in Fig. 1A, but some cells were treated with the Src family kinase inhibitor PP2 or the inactive analog PP3 (10 μM). (D) Cells were stimulated with NO-Cbi as in panel A, but some cells received the MEK/ERK inhibitor U1026 (5 μM). Data represent mean ± SEM of at least 3 separate experiments with n = 12 (C and D); $^{*}p < 0.001$ compared to control, $^{\#}p < 0.001$ and $^{\%}p < 0.001$ for the indicated comparisons.

(Fig. 5C). These data indicate that NO-Cbi's effects on wound healing require Src and MEK/ERK.

## 4. Discussion

The results presented here demonstrate that NO-Cbi accelerates wound healing in several *in vitro* cellular model systems. The method for generating wounds is semi-automated, and hence highly reproducible, yielding uniform wounds. Moreover, we used validated software to analyze the wounds, minimizing variability and maximizing accuracy. Both the wound-generating method and analysis software are easily portable and could be used by other laboratories [26].

We used four different cell types in this study: PtK2 marsupial epithelial cells, A549, adenocarcinomic human basal epithelial cells, NHLF, primary human lung fibroblasts, and U2OS, human osteosarcoma cells. In PtK2 cells, a single application of NO-Cbi was sufficient to significantly improve wound healing, while in the other three cell types several low dose drug applications were necessary. Multiple drug administrations were needed, likely because NO-Cbi has a half-life of about 90 min in tissue culture medium [25]. Studies are in progress on different formulations to increase the half-life of NO-Cbi, however, application of NO-Cbi to a wound three or four times a day would not obviate its potential medical use.

On a molar basis, NO-Cbi more effectively enhanced wound healing than two other direct NO donors, Deta-NONOate and sodium nitroprusside. We compared NO-Cbi to direct NO donors, rather than to indirect NO donors such as nitroglycerin or other organic nitrates, because the latter require cellular biotransformation and can increase production of reactive oxygen species [33,34]. The increased potency of NO-Cbi compared to Deta-NONOate was particularly surprising, because Deta-NONOate releases two nitric oxide molecules per mole of compound. There are several possible explanations for the higher potency of NO-Cbi compared to Deta-NONOate and sodium nitroprusside. First, under the experimental conditions used, the half-life of NO-Cbi could be more favorable for wound healing than that of either Deta-NONOate, which has a half-life of about 20 h at 37 °C [35], or sodium nitroprusside, which has a half-life of less than 30 min [36]. Second, the NO released from NO-Cbi could be biologically more available than that released by the other two drugs. For example, NO-Cbi may enter cells more efficiently than Deta-NONOate and sodium nitroprusside, thereby releasing NO intracellularly rather than extracellularly. Extracellular release of NO into the medium could result in loss either by diffusion into the surrounding air space or by conversion to nitrite and nitrate. Third, the parent compound of the other two NO donors could be toxic, and inhibit wound closure. This was not the case for NO-Cbi, since cobinamide, the parent compound of NO-Cbi, had no effect on wound closure. Sodium nitroprusside could have been toxic to the cells, since it releases five cyanide ions for every NO molecule.

Approximately the same concentration of NO-Cbi was required to enhance wound healing in the four cell types studied. This suggests that the mechanism of action was similar in different cells and that the same amount of NO-Cbi could be used to treat skin and epithelial wounds, as well as other injuries such as bone fractures. Previous studies have shown that NO donors improve fracture healing in animals. In our studies it was effective in U2OS osteosarcoma cells [37]. NO donors improve wound healing in both animals and humans, and intake of the NO synthase substrate L-arginine can improve collagen deposition and wound strength [38]. NO donors may affect wound healing *in vivo* not only by enhancing cell motility, but also by stimulating collagen expression and angiogenesis [39–43].

NO-Cbi did not increase cell proliferation significantly, but it did increase cell migration. Thus, the improved wound healing by this compound was likely a result of cells migrating into the wounded area. Other studies have also shown that NO increases cell migration,

but it can also inhibit motility, depending on the type of cell, level and duration of NO exposure, and assay conditions [44–51].

The pro-migratory effect of NO/cGMP/PKGI on many cell types represents a potential for improved healing. However, high endogenous NO synthesis in human and murine breast cancer cells, promotes migration, since NO synthesis inhibitors inhibit transwell migration of these malignant cells [47,48,52]. Moreover, high expression of NO synthases has been correlated with high tumor grade and presence of lymph node metastases in breast cancer [53–55]. Since cell motility is essential for cancer invasion and metastasis, one must be cautious when using NO donors to enhance wound healing.

IBMX alone improved wound healing, while vardenafil had no effect. This may be because IBMX is a non-specific phosphodiesterase inhibitor, and inhibits phosphodiesterase I–V, VII and XII, while vardenafil specifically inhibits phosphodiesterase V [56,57]. A phosphodiesterase other than PDE V may participate in wound healing, and IBMX increases intracellular cAMP as well as cGMP [58]. cAMP has both positive and negative effects on cell migration, with the variation in results most likely due to the concentration and timing of cAMP application [59,60]. We found no effect of the cAMP analog 8-CPT-cAMP on wound healing in A549 cells.

In this study we have shown that NO-Cbi is a potent new NO-donating drug inducing wound healing in several cell types primarily through enhanced cell migration and not proliferation. Although PKG, ERK, and Src have been shown separately to be involved in wound healing, we are unaware of any studies where the downstream effects of NO were mapped specifically and sequentially. We found that NO enhances wound healing by activating soluble guanylate cyclase, increasing intracellular cGMP, and stimulating PKG, and that PKGI plays a more important role in NO-mediated wound healing than PKGII. Moreover, we showed that MEK/ERK and Src are required for NO-mediated wound healing to proceed. A better understanding of the mechanisms involved in NO-mediated wound closure should result in more effective clinical use of NO donors. NO-Cbi shows significant promise for clinical wound healing applications; work is in progress to create better delivery systems for this purpose.

Supplementary data to this article can be found online at http://dx.doi.org/10.1016/j.cellsig.2013.07.029.

## Acknowledgments

Military Photomedicine Program, AFOSR Grant # FA9550-08-1-0384; CounterACT Program, Office of the Director, National Institutes of Health and the National Institute of Neurological Disorders and Stroke, Grant # U01NS058030.

## References

[1] M.R. Miller, I.L. Megson, British Journal of Pharmacology 151 (3) (2007) 305–321.
[2] I.L. Megson, D.J. Webb, Expert Opinion on Investigational Drugs 11 (5) (2002) 587–601.
[3] P.F. Bove, U.V. Wesley, A.K. Greul, M. Hristova, W.R. Dostmann, A. van der Vliet, American Journal of Respiratory Cell and Molecular Biology 36 (2) (2007) 138–146.
[4] T. Kiviluoto, S. Watanabe, M. Hirose, N. Sato, H. Mustonen, P. Puolakkainen, M. Ronty, T. Ranta-Knuuttila, E. Kivilaakso, American Journal of Physiology. Gastrointestinal and Liver Physiology 281 (5) (2001) G1151–G1157.
[5] M.B. Witte, T. Kiyama, A. Barbul, The British Journal of Surgery 89 (12) (2002) 1594–1601.
[6] G. Han, L.R. Martinez, M.R. Mihu, A.J. Friedman, J.M. Friedman, J.D. Nosanchuk, PLoS One 4 (11) (2009) e7804.
[7] I.M. Wasser, S. de Vries, P. Moenne-Loccoz, I. Schroder, K.D. Karlin, Chemical Reviews 102 (4) (2002) 1201–1234.
[8] P.F. Bove, A. van der Vliet, Free Radical Biology & Medicine 41 (4) (2006) 515–527.
[9] A.J. Gow, D.G. Buerk, H. Ischiropoulos, The Journal of Biological Chemistry 272 (5) (1997) 2841–2845.
[10] R. Radi, Proceedings of the National Academy of Sciences of the United States of America 101 (12) (2004) 4003–4008.
[11] B. Brune, Cell Death and Differentiation 10 (8) (2003) 864–869.
[12] A. Bal-Price, J. Gartlon, G.C. Brown, Nitric Oxide 14 (3) (2006) 238–246.
[13] M. Shichiri, M. Yokokura, F. Marumo, Y. Hirata, Arteriosclerosis, Thrombosis, and Vascular Biology 20 (4) (2000) 989–997.
[14] S.H. Francis, J.L. Busch, J.D. Corbin, D. Sibley, Pharmacological Reviews 62 (3) (2010) 525–563.
[15] T.M. Lincoln, N. Dey, H. Sellak, Journal of applied physiology 91 (3) (2001) 1421–1430.
[16] H. Rangaswami, N. Marathe, S. Zhuang, Y. Chen, J.C. Yeh, J.A. Frangos, G.R. Boss, R.B. Pilz, The Journal of biological chemistry 284 (22) (2009) 14796–14808.
[17] K.T. Ota, V.J. Pierre, J.E. Ploski, K. Queen, G.E. Schafe, Learning & Memory 15 (10) (2008) 792–805.
[18] H. Rangaswami, R. Schwappacher, N. Marathe, S. Zhuang, D.E. Casteel, B. Haas, Y. Chen, A. Pfeifer, H. Kato, S. Shattil, et al., Science Signaling 3 (153) (2010) ra91.
[19] F. Hofmann, The Journal of Biological Chemistry 280 (1) (2005) 1–4.
[20] M. Brenner, S.B. Mahon, J. Lee, J. Kim, D. Mukai, S. Goodman, K.A. Kreuter, R. Ahdout, O. Mohammad, V.S. Sharma, et al., Comparison of cobinamide to hydroxocobalamin in reversing cyanide physiologic effects in rabbits using diffuse optical spectroscopy monitoring, Journal of biomedical optics 15 (1) (2010) 017001.
[21] K.E. Broderick, J. Feala, A. McCulloch, G. Paternostro, V.S. Sharma, R.B. Pilz, G.R. Boss, The FASEB Journal 20 (11) (2006) 1865–1873.
[22] K.E. Broderick, P. Potluri, S. Zhuang, I.E. Scheffler, V.S. Sharma, R.B. Pilz, G.R. Boss, Experimental Biology and Medicine (Maywood, N.J.) 231 (5) (2006) 641–649.
[23] K.E. Broderick, V. Singh, S. Zhuang, A. Kambo, J.C. Chen, V.S. Sharma, R.B. Pilz, G.R. Boss, The Journal of Biological Chemistry 280 (10) (2005) 8678–8685.
[24] W.C. Blackledge, C.W. Blackledge, A. Griesel, S.B. Mahon, M. Brenner, R.B. Pilz, G.R. Boss, Analytical Chemistry 82 (10) (2010) 4216–4221.
[25] K.E. Broderick, L. Alvarez, M. Balasubramanian, D.D. Belke, A. Makino, A. Chan, V.L. Woods Jr., W.H. Dillmann, V.S. Sharma, R.B. Pilz, et al., Experimental Biology and Medicine 232 (11) (2007) 1432–1440.
[26] E.L. Botvinick, M.W. Berns, Microscopy Research and Technique 68 (2) (2005) 65–74.
[27] V.A. Gushchin, Tsitologiia 27 (1) (1985) 107–114.
[28] S.W. Yang, J. Wu, G.X. Luo, X.R. Zhang, X.H. Hu, Y.M. Peng, J.J. Yang, X.L. Luo, Y. Wang, Zhonghua Shao Shang Za Zhi 26 (2) (2010) 146–149.
[29] A. Friebe, D. Koesling, Circulation Research 93 (2) (2003) 96–105.
[30] A. Smolenski, C. Bachmann, K. Reinhard, P. Honig-Liedl, T. Jarchau, H. Hoschuetzky, U. Walter, Journal of biological chemistry 273 (32) (1998) 20029–20035.
[31] J. Liu, C. Huang, X. Zhan, Oncogene 18 (48) (1999) 6700–6706.
[32] P.H. Sugden, A. Clerk, Cellular Signalling 9 (5) (1997) 337–351.
[33] M.V. Wenzl, M. Beretta, A.C. Gorren, A. Zeller, P.K. Baral, K. Gruber, M. Russwurm, D. Koesling, K. Schmidt, B. Mayer, Journal of biological chemistry 284 (30) (2009) 19878–19886.
[34] K. Sydow, A. Daiber, M. Oelze, Z. Chen, M. August, M. Wendt, V. Ullrich, A. Mulsch, E. Schulz, J.F. Keaney Jr., et al., The Journal of Clinical Investigation 113 (3) (2004) 482–489.
[35] L.K. Keefer, R.W. Nims, K.M. Davies, D.A. Wink, Methods in Enzymology 268 (1996) 281–293.
[36] R. Ferrero, F. Rodriguez-Pascual, M.T. Miras-Portugal, M. Torres, British Journal of Pharmacology 127 (3) (1999) 779–787.
[37] S.A. Jamal, C.J. Hamilton, Current Osteoporosis Reports 10 (1) (2012) 86–92.
[38] J.D. Luo, A.F. Chen, Acta Pharmacologica Sinica 26 (3) (2005) 259–264.
[39] G.S. Dhaunsi, P.T. Ozand, Clinical and Experimental Pharmacology & Physiology 31 (1–2) (2004) 46–49.
[40] Y.C. Hsu, M. Hsiao, Y.W. Chien, W.R. Lee, Nitric Oxide 16 (2) (2007) 258–265.
[41] S. Majumder, M. Rajaram, A. Muley, H.S. Reddy, K.P. Tamilarasan, G.K. Kolluru, S. Sinha, J.H. Siamwala, R. Gupta, R. Ilavarasan, et al., British Journal of Pharmacology 158 (7) (2009) 1720–1734.
[42] J.H. Chen, H.H. Lin, T.A. Chiang, J.D. Hsu, H.H. Ho, Y.C. Lee, C.J. Wang, Toxicological Sciences 106 (2) (2008) 364–375.
[43] A. Pyriochou, T. Vassilakopoulos, Z. Zhou, A. Papapetropoulos, Life Sciences 81 (21–22) (2007) 1549–1554.
[44] E. Noiri, E. Lee, J. Testa, J. Quigley, D. Colflesh, C.R. Keese, I. Giaever, M.S. Goligorsky, The American Journal of Physiology 274 (1 Pt 1) (1998) C236–C244.
[45] S. Bulotta, M.V. Ierardi, J. Maiuolo, M.G. Cattaneo, A. Cerullo, L.M. Vicentini, N. Borgese, Biochemical and Biophysical Research Communications 386 (4) (2009) 744–749.
[46] S.K. Gupta, N.E. Vlahakis, Journal of Cell Science 122 (Pt 12) (2009) 2043–2054.
[47] T. Punathil, T.O. Tollefsbol, S.K. Katiyar, Journal of Biochemical and Biophysical Research Communications 375 (1) (2008) 162–167.
[48] L.C. Jadeski, C. Chakraborty, P.K. Lala, International Journal of Cancer 106 (4) (2003) 496–504.
[49] M. Rolli-Derkinderen, G. Toumaniantz, P. Pacaud, G. Loirand, Molecular and Cellular Biology 30 (20) (2010) 4786–4796.
[50] A. Deguchi, W.J. Thompson, I.B. Weinstein, Cancer Research 64 (11) (2004) 3966–3973.
[51] C. Brown, X. Pan, A. Hassid, Circulation Research 84 (6) (1999) 655–667.
[52] R. Schwappacher, H. Rangaswami, J. Su-Yuo, A. Hassad, R. Spitler, D.E. Casteel, Journal of cell science 126 (7) (2013) 1626–1636.
[53] L.C. Jadeski, C. Chakraborty, P.K. Lala, Canadian Journal of Physiology and Pharmacology 80 (2) (2002) 125–135.

[54] L.L. Thomsen, D.W. Miles, L. Happerfield, L.G. Bobrow, R.G. Knowles, S. Moncada, British Journal of Cancer 72 (1) (1995) 41–44.
[55] A. Duenas-Gonzalez, C.M. Isales, M. del Mar Abad-Hernandez, R. Gonzalez-Sarmiento, O. Sangueza, J. Rodriguez-Commes, Modern Pathology 10 (7) (1997) 645–649.
[56] M.A. Blount, A. Beasley, R. Zoraghi, K.R. Sekhar, E.P. Bessay, S.H. Francis, J.D. Corbin, Molecular Pharmacology 66 (1) (2004) 144–152.
[57] R. Zoraghi, J.D. Corbin, S.H. Francis, Journal of biological chemistry 281 (9) (2006) 5553–5558.
[58] I.B. Levitan, J. Norman, Brain Research 187 (2) (1980) 415–429.
[59] A.K. Howe, Biochimica et Biophysica Acta 1692 (2–3) (2004) 159–174.
[60] T.A. Wyatt, J.H. Sisson, M.A. Forget, R.G. Bennett, F.G. Hamel, J.R. Spurzem, Journal of Evidence-Based Medicine 227 (11) (2002) 1047–1053.